Numerical simulation of natural convection heat transfer in a cavity with finned surface under linear temperature profile

Mohamed Tarek ATTOUCHI, Salah LARBI, and Sofiane KHELLADI

Abstract− This paper is dedicated to a numerical study of natural convection through a cavity with finned surface where its base temperature is variable with linear profile. An approach based on modelling of internal fluid flow around a finned surface in laminar and at steady state conditions is used. Thermal and hydrodynamic aspects of the fluid flow were analyzed through the numerical resolution of equations of fluid dynamics. For this purpose, we have developed a computer code (in Fortran 90) based on the finite volume method. The studied model consists of a rectangular cavity where vertical walls are thermally insulated, the horizontal ones are maintained at different temperatures: cold and constant temperature on the upper wall and hot temperature with linear profile on the lower wall. The Rayleigh number used is in the range of 103 to 106 and the Prandtl number is fixed at 0.71. The plotted results are related to temperature distribution, streamlines, velocity fields as well as the mean Nusselt number.

***Keywords*− Natural Convection, Enclosures, Laminar Flow, Fins, Numerical Simulation, Finite Volume Method.**

NOMENCLATURE

a_P, a_E, a_W,a_N and a_S Coefficients associated with variable ϕ
C_P Specific heat at constant pressure, [J/kg.°C]
d Spacing between fins, [m]
g Acceleration due to gravity; [m/s^2]
G_k Term of generation of the turbulent kinetic energy due to the gradient of the mean velocity with: $G_k = -\sqrt{\frac{1}{PrRa}}\frac{\mu_t}{\sigma_T} g\beta \frac{\partial T}{\partial y}$
ENP Ecole Nationale Polytechnique.
ENTR Entropy (Shannon entropy).
DWT Discrete Wavelet Transform.
HV High Voltage.
STD Standard Deviation.
THD Total Harmonic Distortion.
Gr *Grashof* number
H Cavity height, [m]
K Thermal conductivity, [W/m.K]
k Turbulent kinetic energy
L Cavity length, [m]; *l* :fin width, [m]
Nu_L Local *Nusselt* number ,Nu_M :Average *Nusselt* number
P Pressure [Pa]
Pr *Prandtl number;* $Pr = \frac{\nu}{\alpha}$
T Local fluid temperature, [°C]
α Thermal diffusivity, [m^2/s]
β Coefficient of thermal expansion
σ_k; σ_T Turbulent Prandtl number for kinetic and turbulent energy respectively
$\emptyset$ General dependent variable (e.g. temperature, speed, ect.)
ε Energy dissipation rate
ρ Volumic mass, [Kg/m^3]
ν Fluid kinematic viscosity [m^2/s]
μ Fluid dynamic viscosity [kg/(m.s)]
μ_t Turbulent viscosity
ψ Streamlines [m^2/s]
c Cold
h Hot

Manuscript July 31, 2023; accepted December 20, 2023.

M. T. Attouchi, S. LARBI are with the Ecole Nationale Polytechnique, Algiers, ALGERIA (e-mail: mohamed_tarek.attouchi@g.enp.edu.dz, salah.larbi@g.enp.edu.dz)
S. KHELLADI is with Arts et Metiers Institute of Technology, CNAM, LIFSE, HESAM University, Paris, FRANCE (e-mail: sofiane.khelladi@ensam.eu).

Digital Object Identifier (DOI): 10.53907/enpesj.v3i2.223

I. INTRODUCTION

Heat transfer by natural convection, in enclosures with finned surfaces and under differential heating conditions, is of primary importance in many engineering applications. It is encountered in various fields of industrial applications, such as the cooling devices of electronic instruments, the operation of safety of nuclear reactors, the solar collectors, the boilers, the fire fighting, the energy storage systems, the radioactive waste storage, the energy efficiency of buildings. Many researchers have conducted the studies related to the various aspects of this problem theoretically and experimentally. In the following, we present a bibliographical study allowing us to make a synthesis of research work based essentially on cavities with finned surfaces and subjected to different boundary conditions.

W. S. Fu and W. J. Shieh [1] carried out a theoretical study of natural convection in a square enclosure partitioned by a single adiabatic fin attached to the ceiling wall. The Rayleigh numbers considered are 104 and 105. The results showed that the heat transfer coefficients were influenced by the height and the location of the fin.

M. H. Novak and E. S. Nowak [2] used the CAV computer code for a 2D numerical analysis of natural convective laminar heat transfer and fluid flow distribution in rectangular and square thin-windowed cavities with or without inner fins. Recommendations on window design were made. The numerical analysis carried out by I. Dagtekin and H.F. Oztop [3], was based on the study of heat transfer by natural convection and the flow of the fluid in an enclosure equipped with two heated fins. The right and lower sidewalls were perfectly insulated, while the left and upper ones were kept at the same uniform temperature. The fins were placed at the bottom of the enclosure with higher temperatures than that of the uninsulated walls. The effects of the position and the height of the fins on the heat transfer and the flow field as well as the average Nusselt number were studied.

N. Yucel and A. H. Ozdem [4] numerically studied fluid flow and heat transfer in partially divided square enclosures, the horizontal end walls of the enclosure were chosen adiabatic and the left and right side walls were maintained at uniform, but different temperatures and were subjected to appropriate boundary conditions and a Rayleigh number range of 103 to 5.105. It has been observed that, the average Nusselt number increases with increasing Rayleigh number and decreases with increasing number of partitions, however, the decrease in average Nusselt number is apparent at low Rayleigh numbers. Note that the increase in the height of the partition induces a decrease in the average Nusselt number.

E. Bilgen [5] carried out a numerical study on differentially heated square cavities. The horizontal walls are adiabatic while the vertical ones are isothermal. A thin fin is attached to the active wall. It was found that the Nusselt number increases with increasing Rayleigh number and decreases with increasing fin length. However, there is an optimum fin position, often at or near the center of the cavity, to minimize heat transfer by natural convection.

A. F. Fahaid [06] has numerically studied laminar natural convection in vertical enclosures fitted with conductive fins attached to the hot vertical wall. The side vertical walls were kept at constant but different temperatures, while the horizontal wall and the bottom wall were kept adiabatically. It has been observed that the rate of heat transfer through an enclosure is largely affected and therefore it can be controlled by the number of fins attached to the vertical sidewall of the enclosure, as well as the fin lengths.

A. Ben-Nakhi and A.J. Chamkha [7] have numerically examined natural convection in steady and laminar regimes in a square enclosure with a thin inclined fin of arbitrary length and perfectly conducting. The fin is attached to the hot vertical left wall, while the other three cold walls are thick, of the same thickness, and of arbitrary thermal conductivity. The results showed the effects of the angle of inclination of the thin fin on the length and the thermal conductivity of the surfaces concerned.

A. Al Amiri and K. Khanafer [8] presented a study, which deals with the buoyancy induced by the heat transfer in a partially divided square enclosure. The Rayleigh number is taken in the range: $104 \leq Ra \leq 107$. The results revealed that all parameters related to the geometric dimensions of the heating element significantly affect the flow field, isotherms and heat transfer. The study revealed that increasing the heat exchange surface of the heating element, increasing its height, width and location improved heat transfer.

A.F. Costa [9] has numerically studied natural convection in a square, partitioned, air-filled enclosure. Two fins of finite thickness are placed in the enclosure, whose position, length and thermal conductivity vary both as a function of the Rayleigh number and as a function of the boundary conditions. The overall thermal performance of the enclosure was analyzed through the Nusselt number.

F. Selimefendigil and H. F. Öztop [10] conducted a numerical study on the heat transfer from a square cavity in the presence of an adiabatic and tilted thin fin. The upper and lower walls of the cavity were maintained at a constant temperature, while the vertical ones are assumed adiabatic. The average Nusselt number was determined as a function of the height of the fin, its angle of inclination and the Richardson number.

C. Benseghir and S.Rahal [11] carried out a numerical study of transient laminar natural convection in a square cavity differentially heated and filled with air. Thin rectangular fins made with a high conductivity material were placed on the hot wall of the cavity. A single value of Rayleigh Ra=105 was considered. This study highlights the existence of an optimal length of the fins allowing the maximization of the natural convection on the cold wall.

S. G. Martyusheva, M. A. Sheremeta [12] performed a two-dimensional numerical analysis of the combined heat transfer (transient natural convection, thermal radiation and conductive surface). The enclosure concerned is square and filled with air. The walls, solid and conductive, have a finite thickness and a local heat source with conditions of heat exchange by convection with the surrounding environment.

It was found that, the average Nusselt number increases with the Rayleigh number and the thermal conductivity ratio. However, it decreases with surface emissivity and the ratio of wall thickness to cavity spacing. It is important to note that the above investigations consider constant hot and cold temperatures in the study of natural convection in finned enclosures. The novelty of our work lies in (i) the consideration of a linear temperature profile at the level of the fins, (ii) the adoption of our own boundary conditions, (iii) the presentation of the velocity fields not plotted in the research aroused. Indeed, the main objective of the present study is to analyze the natural convection in laminar and permanent regimes in a square enclosure equipped with fins heated in a non-uniform way according to a linear temperature profile. A careful analysis of the effect of the heating elements on the heat transfer inside the cavity will be carried out by imposing well-defined boundary conditions, for various parameters, namely the Rayleigh number, the Prandtl number, the height and fin width and number of heating elements.

II. PHYSICAL MODEL

The physical model considered is shown in Figure 1. It is a cavity of length L and height H.

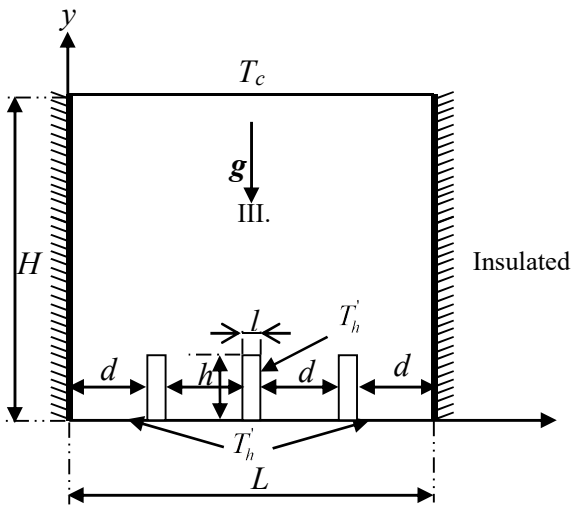

Fig. 1: Schematic representation of the physical model used.

The vertical walls are thermally insulated. As for the horizontal walls of the enclosure, they are maintained at different temperatures T_c and T_h'.

Identical fins, of thickness l and height h, are placed equidistantly on the lower wall of the cavity and maintained at

a temperature T_h' such that*h/H = 1/5*and its width *l/L = 1/20*.The heat transfer in the cavity is done by natural convection and the Prandtl number is 0.71. The vector g represents the acceleration due to gravity.

III. MATHEMATICAL MODEL

A dimensionless form of the equations reduces the number of independent parameters in the equations and makes the solutions more general for a given set of parameters. It helps to save machine time by increasing the convergence speed of the solution.
The dimensionless equations are derived in such a way that only the Prandtl and Rayleigh numbers of the fluid are dimensionless parameters.

A. Governing equations

The mathematical model used is based on the classical equations of conservation balances (mass, momentum and energy), is given by equations (1), (2), (3) and (4).
- For the mass balance equation:

$$\frac{\partial \rho}{\partial t}+\frac{\partial(\rho u)}{\partial x}+\frac{\partial(\rho v)}{\partial y}=0 \quad (1)$$

- For the momentum balance equation along the *x* direction:

$$\rho\frac{\partial u}{\partial t}+\rho u\frac{\partial u}{\partial x}+\rho v\frac{\partial u}{\partial y} = -\frac{\partial P}{\partial x}+\sqrt{\frac{Pr}{Ra}}\frac{\partial}{\partial x}\left[(\mu+\mu_t)\left(2\frac{\partial u}{\partial x}\right)\right] + \sqrt{\frac{Pr}{Ra}}\frac{\partial}{\partial y}\left[(\mu+\mu_t)\left(\frac{\partial u}{\partial y}+\frac{\partial v}{\partial x}\right)\right] \quad (2)$$

- For the momentum balance equation along the y direction:

$$\rho\frac{\partial v}{\partial t}+\rho u\frac{\partial v}{\partial x}+\rho v\frac{\partial v}{\partial y}=-\frac{\partial P}{\partial y}+\sqrt{\frac{Pr}{Ra}}\frac{\partial}{\partial y}\left[(\mu+\mu_t)\left(2\frac{\partial v}{\partial y}\right)\right]+ \sqrt{\frac{Pr}{Ra}}\frac{\partial}{\partial x}\left[(\mu+\mu_t)\left(\frac{\partial u}{\partial y}+\frac{\partial v}{\partial x}\right)+(T-T_{ref}\right] \quad (3)$$

- For the energy balance equation:

$$\rho\frac{\partial T}{\partial t}+\rho u\frac{\partial T}{\partial x}+\rho v\frac{\partial T}{\partial y}=\frac{1}{\sqrt{PrRa}}\frac{\partial}{\partial x}\left[\left(\mu+\frac{\mu_t Pr}{\sigma_T}\right)\frac{\partial T}{\partial x}\right]+ \frac{1}{\sqrt{PrRa}}\frac{\partial}{\partial y}\left[\left(\mu+\frac{\mu_t Pr}{\sigma_T}\right)\frac{\partial T}{\partial y}\right] \quad (4)$$

The governing equations given by the relations (1) to (4) with their corresponding boundary conditions are given in a dimensionless form in order to generalize the study. It should also be noted that the terms of turbulence and those dependent on time are not taken into account in this study. We define the expressions of the speed as a function of the current function as:

$$v=-\frac{\partial \psi}{\partial x};u=\frac{\partial \psi}{\partial y}$$

Consider u^* and v^*, T^*, P^*, x^* and y^*, the dimensionless forms of the components of velocity vectors, temperature, pressure and space variables:

$$u^*=\frac{u}{u_{ref}}=\frac{u}{\sqrt{g\beta H\Delta T}};v^*=\frac{v}{v_{ref}}=\frac{v}{\sqrt{g\beta H\Delta T}};T^*=\frac{T-T_c}{T_h-T_c};\ P^*=\frac{P}{P_{ref}};\ x^*=\frac{x}{L};\ y^*=\frac{y}{H}$$
$$\psi^*=\frac{\psi}{\alpha};\ T_{ref}=\frac{T_h+T_c}{2};\ \Delta T=T_h-T_c$$
$$u_{ref}=v_{ref}=\sqrt{g\beta H\Delta T};\ P_{ref}=\rho u_{ref}^2$$

The index *ref* represents the reference value for all the variables.
T_c: is the cold temperature; T_h: hot temperature.
The temperatures $T_h$and $T_c$become equal to 1 and 0 on a dimensionless scalar.
The local Nusselt number at the hot wall is given by:

$$Nu_L=-\frac{L}{\Delta T}\frac{\partial T}{\partial y}\Big|_{x^*=0}$$

While the average Nusselt number is represented by:

$$Nu_M=-\frac{L}{\Delta T}\int\left(\frac{\partial T}{\partial y}\right)_{x^*=0}dx$$

B. Numerical Scheme and Solving Method

The final form of the general two-dimensional discretization equation is written:

$$a_P\phi_P=a_W\phi_W+a_E\phi_E+a_S\phi_S+a_N\phi_N+b \quad (5)$$

with

$$a_E=D_eA(|P_e|)+\mathrm{Max}[-F_e,0]$$
$$a_W=D_wA(|P_w|)+\mathrm{Max}[F_w,0]$$
$$a_N=D_nA(|P_n|)+\mathrm{Max}[-F_n,0]$$
$$a_S=D_sA(|P_s|)+\mathrm{Max}[F_s,0]$$

with

$$A(|P_i|)=Max[0,(1-0.1|P|)^5]$$

According to the power law used in this calculation,

$$b=S_C\Delta x\Delta y+a_P^0\phi_P^0+M$$
$$a_P=(a_W+a_E+a_N+a_S)+\Delta F+(a_P^0-S_p\Delta x\Delta y)$$
$$\Delta F=F_e-F_w+F_n-F_s$$
$$a_P^0=\frac{\rho_P^0\Delta x\Delta y}{\Delta t}$$

F**:** The convection force or mass flow through the interfaces of the control volumes;
D: Diffusion conductance and $P=\frac{F}{D}$ (Number of *Peclet*), with

$$F_e=(\rho u)_e\Delta y;\ F_w=(\rho u)_w\Delta y$$
$$F_n=(\rho v)_n\Delta x;F_s=(\rho v)_s\Delta x \quad (6)$$
$$D_e=\frac{\Gamma_e\Delta y}{(\delta x)_e}=\frac{(\mu+\mu_t)_e}{(\delta x)_e};\ D_w=\frac{\Gamma_w\Delta y}{(\delta x)_w}=\frac{(\mu+\mu_t)_w}{(\delta x)_w}$$
$$D_n=\frac{\Gamma_n\Delta x}{(\delta y)_n}=\frac{(\mu+\mu_t)_n}{(\delta y)_n};D_s=\frac{\Gamma_n\Delta x}{(\delta y)_s}=\frac{(\mu+\mu_t)_s}{(\delta y)_s} \quad (7)$$
$$P_e=\frac{F_e}{D_e};\ P_w=\frac{F_w}{D_w};\ P_n=\frac{F_n}{D_n};\ P_s=\frac{F_s}{D_s} \quad (8)$$

M: Modification to momentum equations

$$M=[\sqrt{\frac{Pr}{Ra}}\frac{\partial}{\partial x}\left[(\mu+\mu_t)\left(\frac{\partial u}{\partial x}+\frac{\partial v}{\partial y}\right)\right]$$

($M=0$ for incompressible fluids where the density does not change with time).

IV. NUMERICAL RESOLUTION

Governing equations, from (1) to (4), were used in their dimensionless form in the calculation with the aim of reducing the number of independent parameters in the equations and making the solutions more general for a data set of parameters in a concern for gain in machine time by increasing the speed of convergence of the solution. The characteristic dimensionless numbers are those of Prandtl and Rayleigh. The numerical modeling of the problem was established through the resolution of fluid dynamics equations, using the finite volume method with adequate boundary conditions. The power law scheme is chosen and used in this calculation, the Rayleigh numbers also used are in the range $10^3 \leq Ra \leq 10^6$, while the Prandtl number is taken equal to Pr=0.71. The mesh grids used in the calculation are of different sizes depending on the geometry of the cavity, ranging from 102 × 102 up to 302 × 302. They are regular in the temperature calculation and are staggered for the speed calculation. A convergence test of an order taken in an interval:

$10^{-2} \leq \varepsilon \leq 10^{-4}$ based on the residuals of T, u and v, is applied in this calculation as follows:

$$\emptyset^{(n)} - \emptyset^{(n-1)} = \varepsilon$$

V. BOUNDARY CONDITIONS

The boundary conditions used for solving the governing equations, (1) to (4), are related to the non-slip condition for the velocity and the Dirichlet or Newman condition for the temperature. The fins are heated at non-uniform temperature, T_h' given by

$$T_h' = T_h - (T_h - T_c)\frac{x}{L}$$

For temperature, the dimensionless boundary conditions are:
Bottom wall:

$-T^*(x^*, 0) = 1 - x^*$ for the variable hot temperature at the level of the fins and on the rest of the wall.

Top wall:

$-T^*(x^*, 1) = 0$ is a constant cold temperature.

- $\frac{\partial T^*}{\partial x^*}(0, y^*) = 0$ on the left wall.

- $\frac{\partial T^*}{\partial x^*}(1, y^*) = 0$ on the right wall.

* For velocities and stream functions:
$-u^*(0,y^*)=u^*(1,y^*)=0$; $u^*(x^*,0)=u^*(x^*,1)=0$
and $v^*(0,y^*)=v^*(1,y^*)=0$; $v^*(x^*, 0)=v^*(x^*,1)=0$
$-\psi^*(0,y^*)=\psi^*(1,y^*)=0$; $\psi^*(x^*, 0)=\psi^*(x^*,1)=0$
$-u^*=v^*=\psi^*=0$ at the fins.

- A regular mesh (figure 2-a) is used for the calculation of the pressure fields, and of the temperature.

- A staggered mesh whose nodes are located halfway from those of the main mesh, as shown in figure 2-(b,c) to calculate the horizontal u and vertical v components of the velocity. Each component of the velocity is staggered according to its direction.

Mesh generating functions

In the problem presented above, a sine function is used to produce the mesh in the *x* and *y* directions for the single cavities This function can be expressed mathematically as

$$\frac{xu(i)}{H} = \frac{i-2}{imax} - \frac{1}{2\pi}sin\left(2\pi\frac{i}{imax}\right) i = imin, imax$$
$$\frac{yv(i)}{H} = \frac{j-2}{jmax} - \frac{1}{2\pi}sin\left(2\pi\frac{j}{jmax}\right) \quad j = jmin, jmax$$

with *imin=jmin=2, imax=NI-2*, and *jmax=NJ-2*

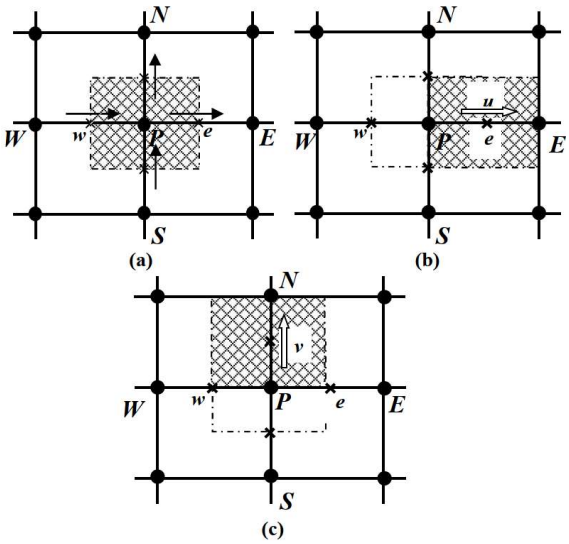

(c)

Fig. 2: Storing used parameters
(a) Storage of pressure and temperature P,T
(b) Storage of horizontal velocity u
(c) Storage of vertical velocity v

The sine function generates a non-uniform mesh that is carefully spaced near the wall and sparsely far away from the wall.
For the cavities equipped with fins, it is preferred to use a uniform mesh defined as follows:

$$\frac{xu(i)}{H} = \frac{i-2}{imax}; \; i = imin, imax$$
$$\frac{yv(i)}{L} = \frac{j-2}{jmax}; \; j = jmin, jmax$$

VI. CODE VALIDATION

The developed computer code is validated by the Benchmark solutions relating to the problem of natural convection in a differentially heated square cavity under different Rayleigh numbers [22].
For the validation of the numerical code without the presence of fins case, the results of references [14, 15] correspond to a closed square cavity whose left and right vertical walls are differentially heated, while the horizontal walls are adiabatic.
The validation of the computer code in the case of finned surface is done [22]. The results of reference [8] correspond to a closed square cavity. The bottom wall is characterized by the presence of an obstacle, while the left and right vertical walls are maintained at a constant cold temperature T_c, while the walls horizontals are maintained adiabatic, the isothermal obstacle is maintained at a constant temperature T_h and is placed at a well determined distance from the right and left wall. Table 1 gives the results comparison between our results for maximum, minimum and average Nusselt number with those of

the literature review for a cavity without fins under the same operating conditions.

VII. RESULTS PRESENTATION

The cavity model used in the computer code where the dimension les height and width of the fin equal respectively h/H=1/5 ,*l*/*L*=1/20, the distance between fins is:
d/*L*=((*L*-*N*×*l*)/(*N*+1))/*L* for *N* fins.
We take*: Pr*=0.71 , T_h' variable and $10^3 \leq Ra \leq 10^6$

***Case of a cavity without fins**

With linear temperature profile: $T_h' = T_h - (T_h - T_c)\frac{x}{L}$

The results are plotted in the form of isotherms, current functions and iso-velocities *u* e *v* respectively.

The contours of isotherms, iso-currents and iso-velocities *u* and *v*, as well as the local Nusselt number as function of the Rayleigh number of the top wall and the bottom wall are plotted respectively for the Rayleigh values:10^3,10^4,10 and10^6 :
Figure 3 illustrates the isotherms, the streamlines and the iso-velocity contours (u and v) for *Pr*=0.71 and *Ra*=10^3 respectively and without fins.

- Linear heating of the bottom wall without fins

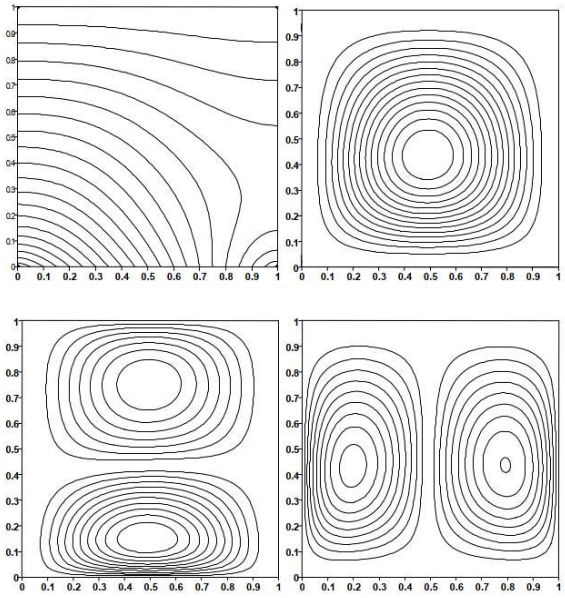

Fig. 3: Results for a finless cavity at Ra=10^3
Linear heating of the bottom wall without fins

Figures (4-a and 4-b) show the local Nusselt number for top and bottom wall for *Pr*=0.71 and *Ra*=10^3respectively and without fins.

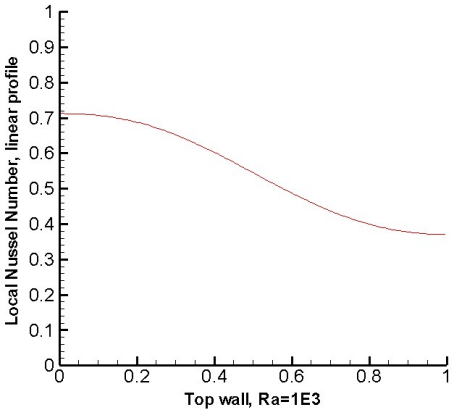

Fig. 4-a: Local Nusselt number
Top wall, for a finless cavity at Ra=10^3

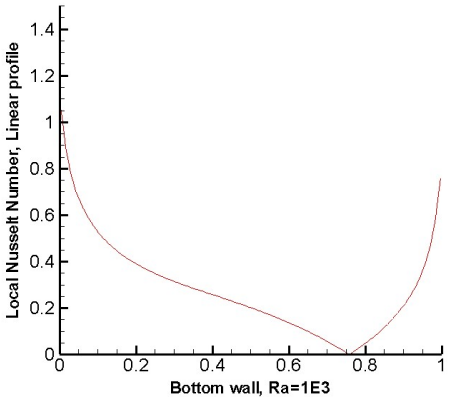

Fig. 4-b: Local Nusselt number
bottom wall, for a finless cavity at Ra=10^3

Table 1. Results comparison between the present study and those of the literature review

Ra	*Nus*	[16]	[17]	[18]	[19]	[20]	[21] FEM-DSC	**Present study**
10^3	Max	1.50	-	-	1.47	1.5062	1.501-1.444	**1.506**
	Min	0.692	-	-	0.623	0.6913	0.691-0.665	**0.697**
	Moy	1.12	-	1.117	1.074	-	1.117-1.073	**1.1008**
10^4	Max	3.53	3.5	-	3.47	3.5305	3.576-3.441	**3.535**
	Min	0.586	-	-	0.497	0.5850	0.577- 0.528	**0.605**
	Moy	2.243	-	2.243	2.084	-	2.254-2.155	**2.225**
10^5	Max	7.71	7.71	-	7.71	7.7084	7.945- 7.662	**7.724**
	Min	0.729	-	-	0.614	0.7282	0.698- 0.678	**0.784**
	Moy	4.52	-	4.521	4.3	-	4.598 – 4.352	**4.486**
10^6	Max	17.92	17	-	17.46	17.5308	17.86- 17.39	**17.4912**
	Min	0.989	-	-	0.716	0.9845	0.9132-	**1.185**
	Moy	8.8	-	8.806	8.743	-	0.903	**8.7268**
							8.976- 8.632	

**** Case of a cavity with fins**

Figure 5 illustrates the isotherms, the streamlines and the iso-velocity (u and v) contours for different fin numbers (N=1, 2, 3, 5, 7) with h/H=0.20, w/W=0.05 and for: *Pr*=0.71 and *Ra*=10^3.

-Case of a one fin

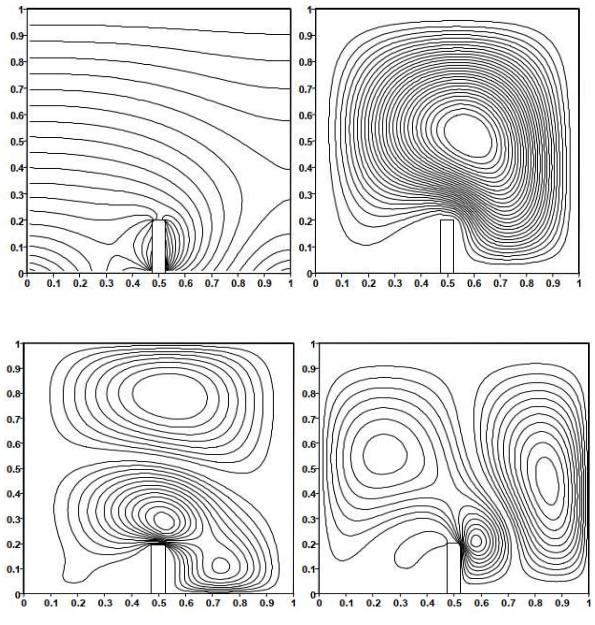

-Case of two fins

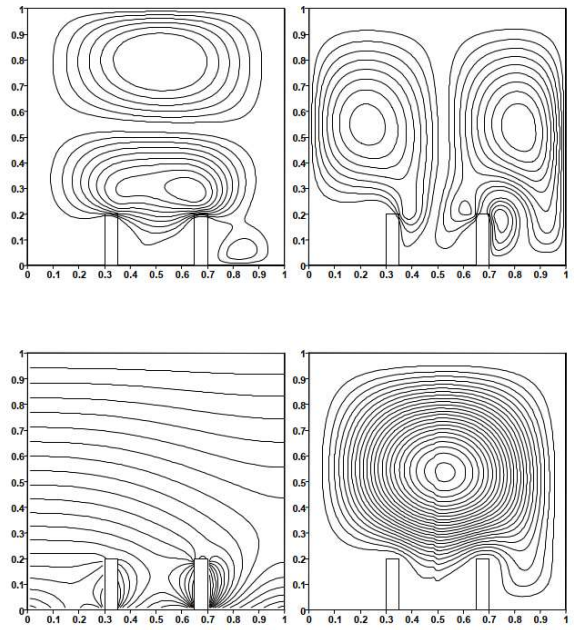

-Case of three fins

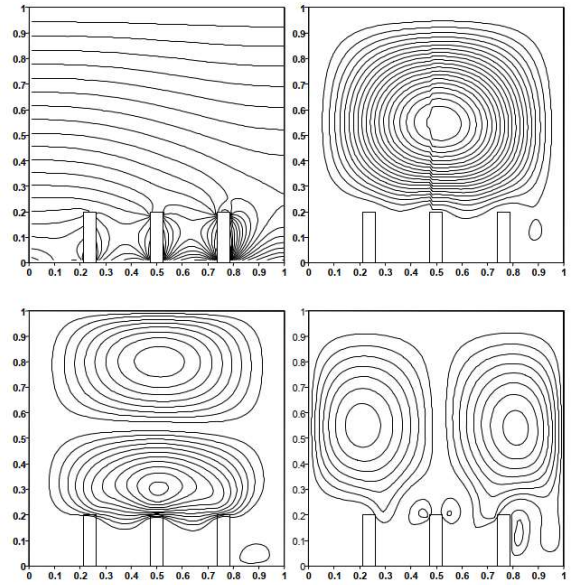

-Case of five fins

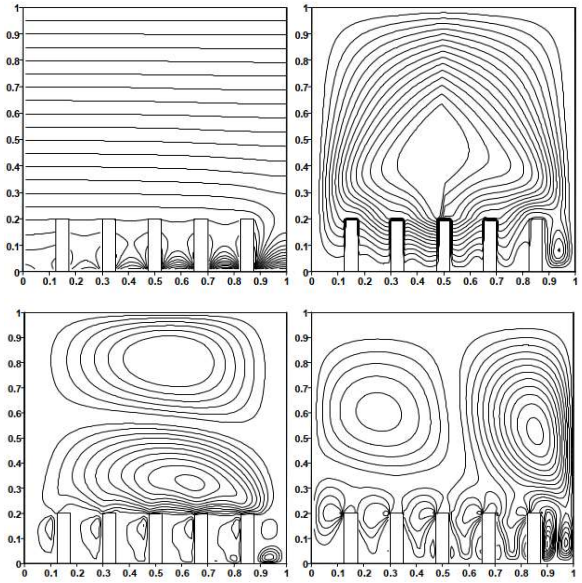

-Case of seven fins

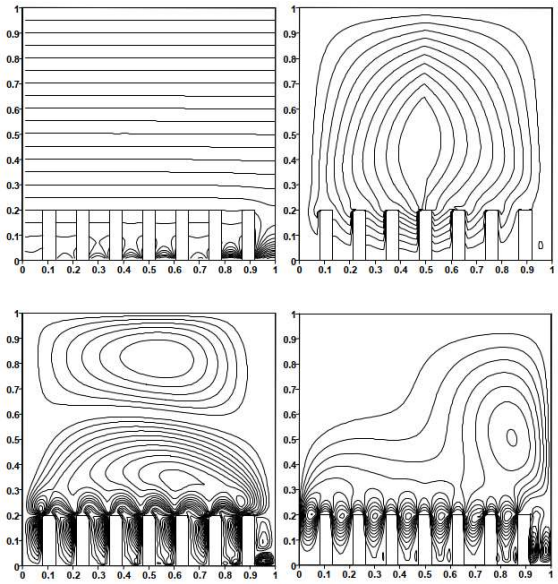

Fig. 5: Results for a finned cavity at Ra=10^3

Figure 6 illustrates the isotherms, the streamlines and the iso-velocity contours (u and v) for Pr=0.71 and Ra=10^4 respectively without fins.

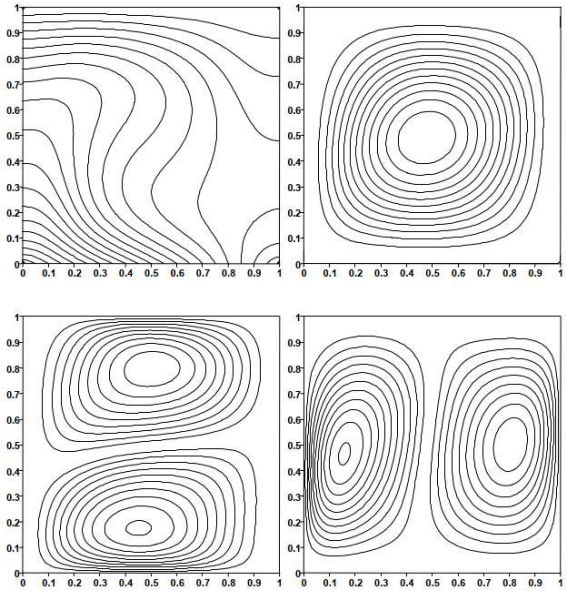

Fig. 6: Results for a finless cavity at Ra=10^4

Figures (7-a and 7-b) show the local Nusselt number for top and bottom wall for Pr=0.71 and Ra=10^4 respectively without fins.

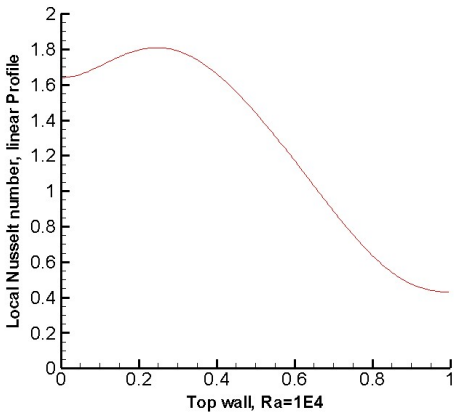

Fig. 7-a: Local Nusselt number
Top wall, for a finless cavity at Ra=10^4

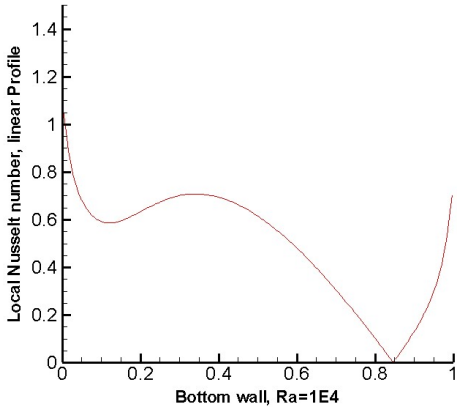

Fig. 7-b: Local Nusselt number bottom wall, for a finless cavity at $Ra=10^4$

Figure 8 illustrates the isotherms, the streamlines and the iso-velocity (u and v) contours for different fin numbers (N=1, 2, 3, 5, 7) with h/H=0.20, w/W=0.05 and for: Pr=0.71 and $Ra=10^4$.

-Case of a one fin

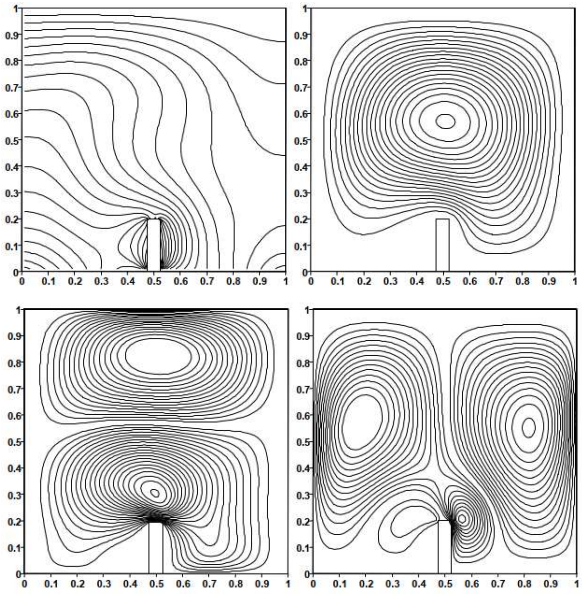

-Case of two fins

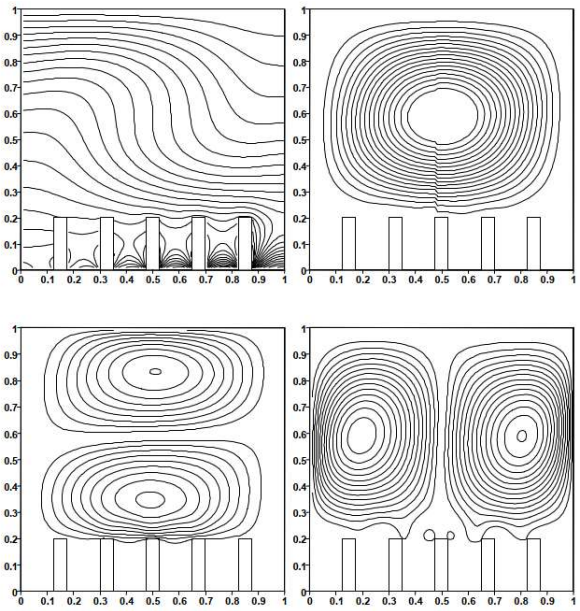

-Case of seven fins

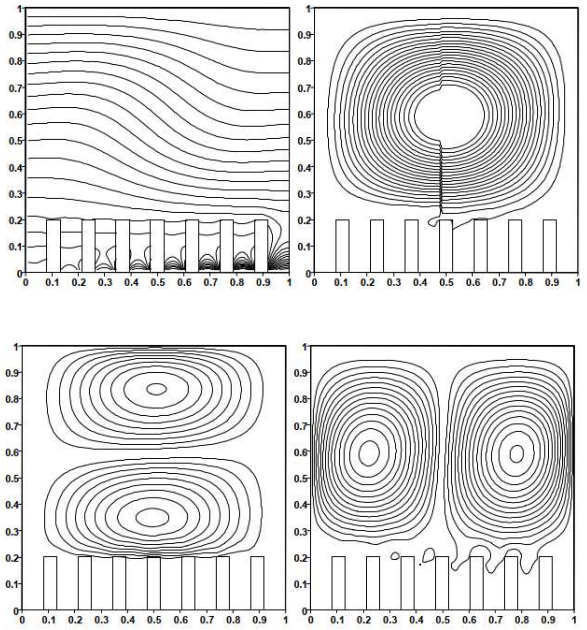

Fig. 8: Results for a finned cavity at Ra=10^4

Figure 9 shows the isotherms, the streamlines and the iso-velocity contours (u and v) for Pr=0.71 and $Ra=10^5$ respectively without fins.

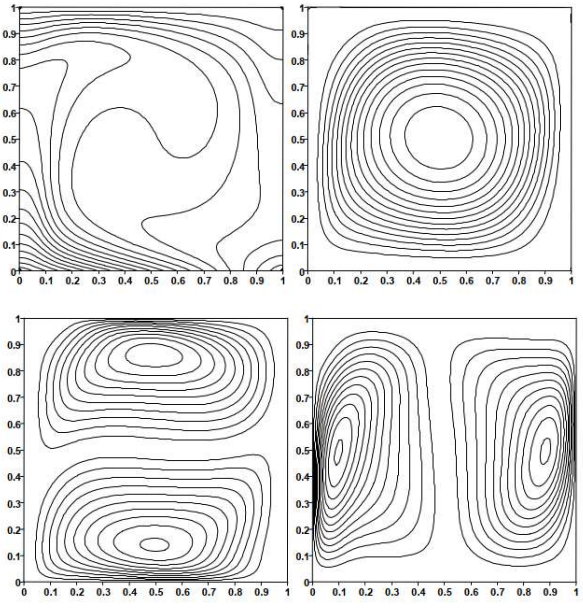

Fig. 9: Results for a finless cavity at Ra=10^5

Figures (10-a and 10-b) illustrate the local Nusselt number for top and bottom wall for Pr=0.71 and $Ra=10^5$, respectively without fins.

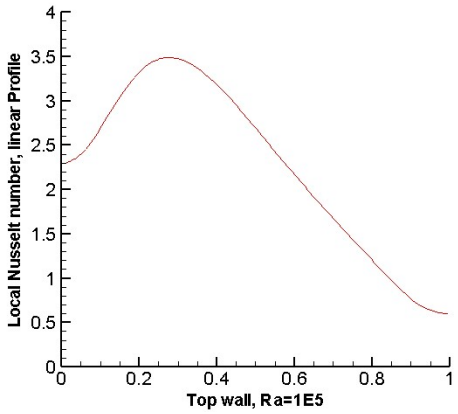

Fig. 10-a: Local Nusselt number
Top wall, for a finless cavity at Ra=10^5

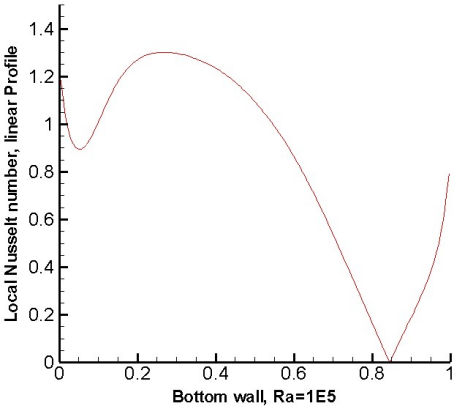

Fig. 10-b: Local Nusselt number
bottom wall, for a finless cavity atRa=10^5

Figure 11 shows the isotherms, the streamlines and the iso-velocity (u and v) contours for different fin numbers (N=1, 2, 3, 5, 7) with h/H=0.20, w/W=0.05 and for: *Pr*=0.71 and *Ra*=10^5.

-Case of one fin

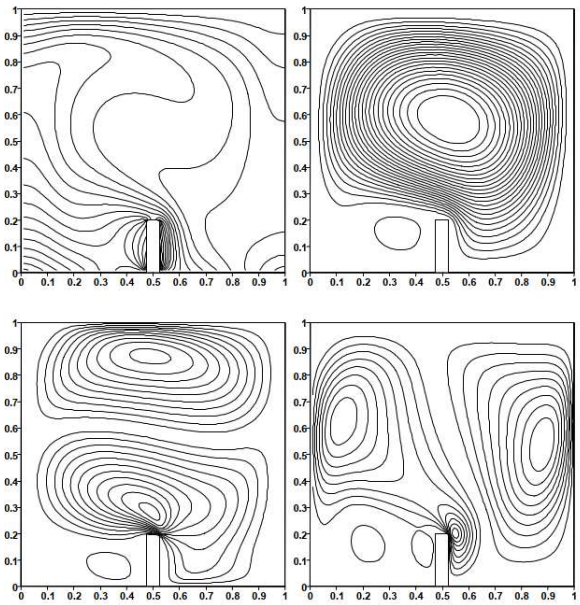

-Case of two fins

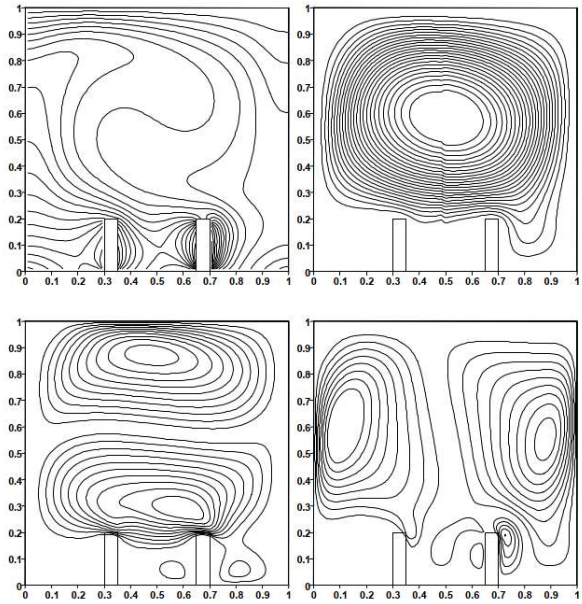

-Case of three fins

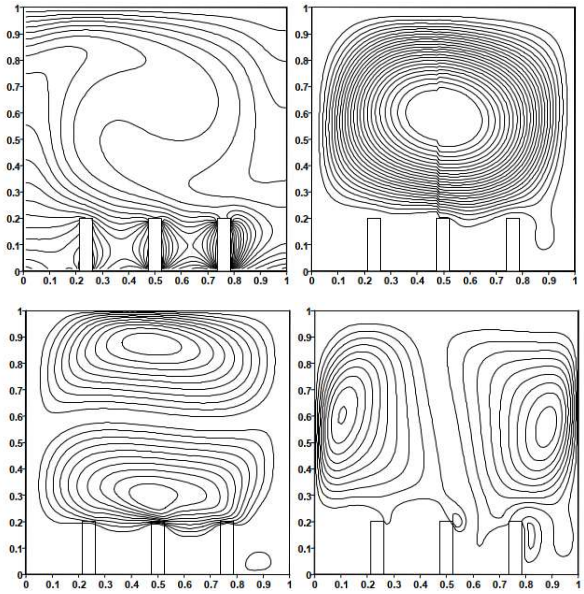

-Case of five fins

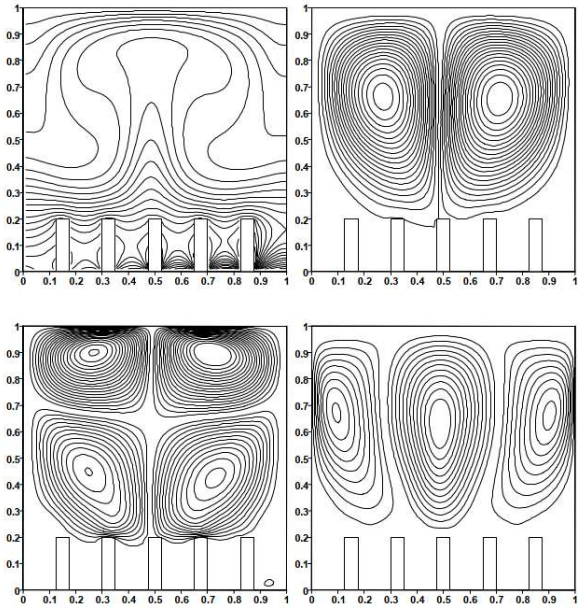

-Case of seven fins

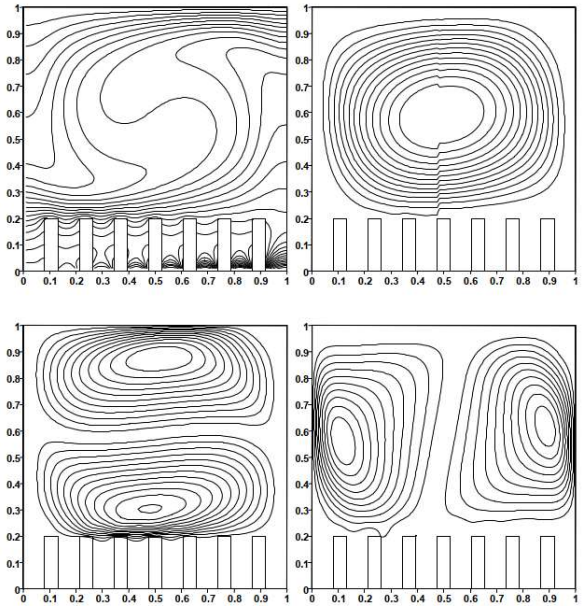

Fig. 11: Results for a finned cavity at Ra=10^5

Figure 12 illustrate the isotherms, the streamlines and the iso-velocity contours (u and v) for *Pr*=0.71 and *Ra*=10^6 respectively without fins.

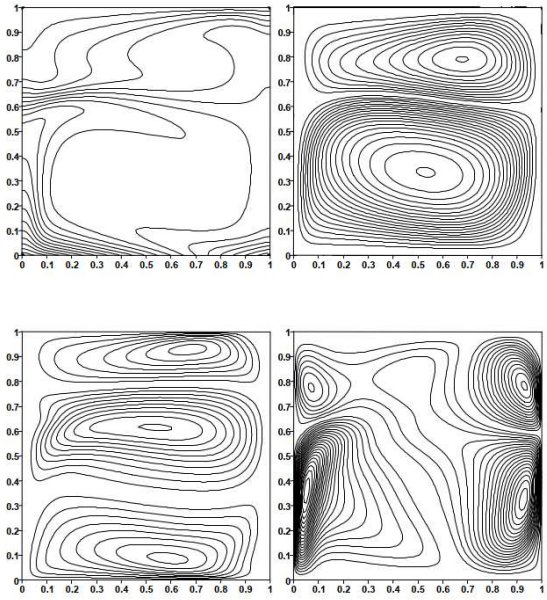

Fig. 12: Results for a finless cavity at Ra=10^6

Figures (13-a and 13- b) show the evolution of the local Nusselt number for top and bottom wall for *Pr*=0.71 and *Ra*=10^6respectivelywithout fins

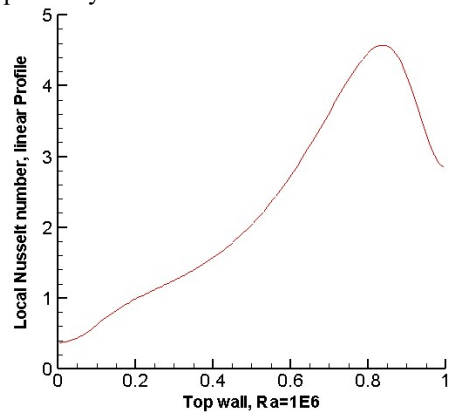

Fig.13-a: Local Nusselt number
Top wall, for a finless cavity at Ra=10^6

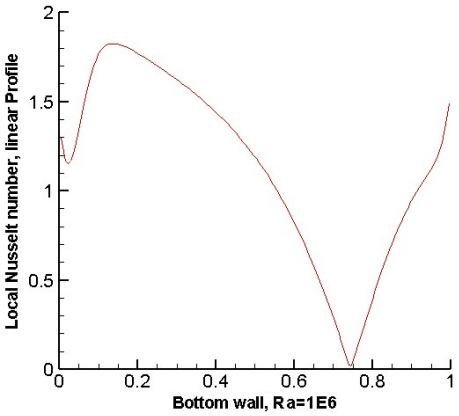

Fig.13-b: Local Nusselt number
bottom wall, for a finless cavity atRa=10^6

Figure 14 illustrates the isotherms, the streamlines and the iso-velocity (u and v) contours for different fin numbers (N=1, 2, 3, 5, 7) with h/H=0.20, w/W=0.05 and for: *Pr*=0.71 and *Ra*=10^6

-Case of one fin

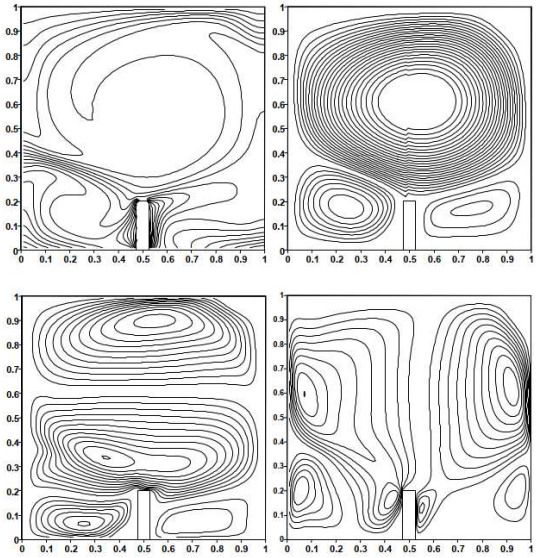

-Case of two fins

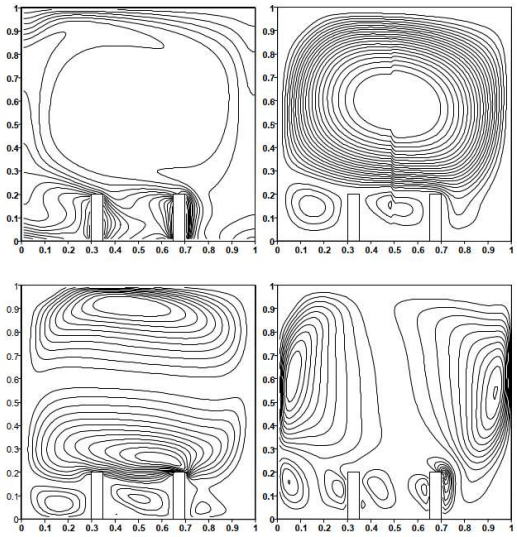

-Case of three fins

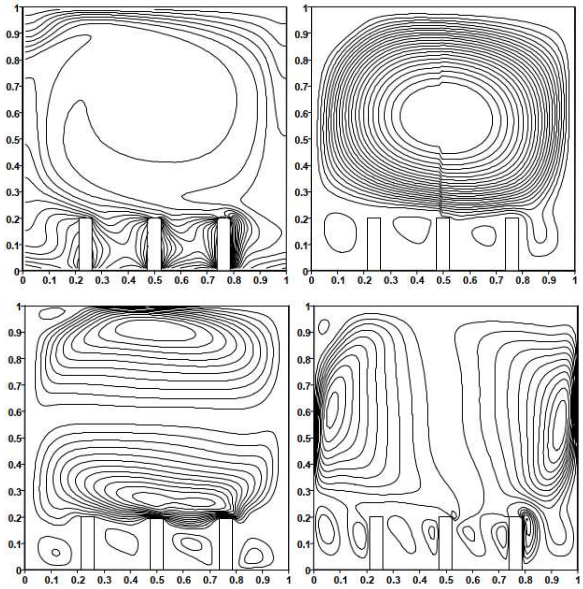

-Case of five fins

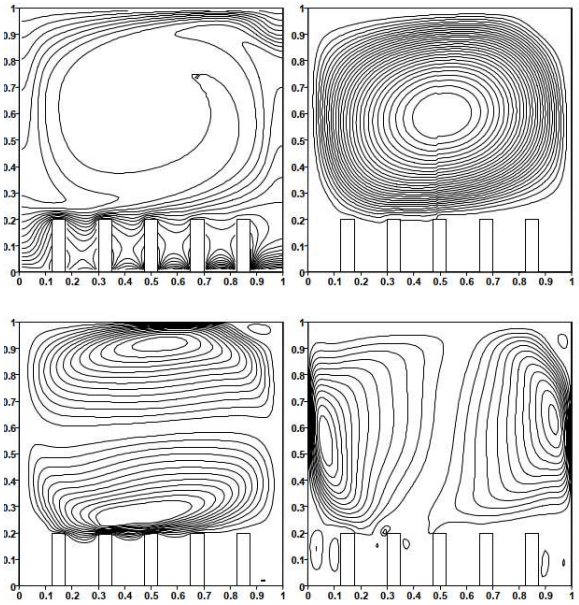

-Case of seven fins

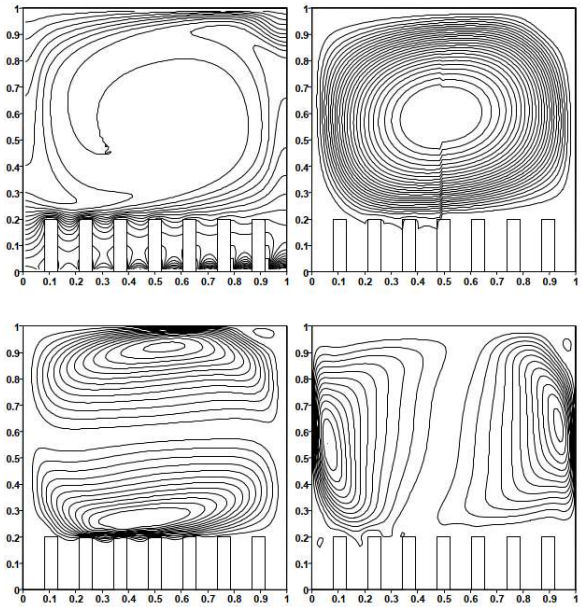

Fig. 14: Results for a finned cavity at Ra=10^6

VIII. DISCUSSIONS

***Linear heating of the bottom wall without fins**

The contours of the isotherms, of the current functions, as well as the iso-velocities for Ra = 10^3-10^6 and Pr = 0.71 are represented in figures (3), (6), (9) and (12). When the bottom wall is heated in a non-uniform and linear manner, the non-uniform heating suppresses singularities at the edges of the bottom wall and exhibits an even temperature distribution throughout the cavity.

For Ra = 10^3, the thermal boundary layer develops only over 60% of the cavity (figures 3). It is observed in the vicinity of Ra=10^4, it can be noted that the temperature at the bottom wall is not uniform and a temperature maximum occurs(Figure 6), at the center, therefore, higher rates of heat transfer occur in the center.

At Ra = 10^5, the circulation model is qualitatively similar to the uniform heating case (Figure 9).

Due to non-uniform bottom heating, the heating rate near the wall is generally lower, which induces less buoyancy resulting in a lower thermal gradient throughout the domain. The uniformity of the temperature distribution and the temperature gradient are even less observed on the regime of the central part inside the upper half of the domain. The effect of lower buoyancy also leads to a large area of temperature stratification at the vertical line of symmetry.

From Ra = 10^6, the mechanism of convection becomes more pronounced and consequently the central vortex moves upwards. Figure (12) also shows that the isotherms are horizontal and vertical inside enclosure; the boundary layers become very thin, this can be attributed to a current inside the cavity, which also causes a reduction in temperature gradients in the center of the cavity at high convection.

The contours of the iso-velocities reveal several important characteristics, in the contours of the iso-velocities-u, for the values of Ra=10^3,10^4,10^5 and 10^6, we notice four horizontal vortices, which form, two below the two others. For the contours of the iso-velocity-v, if we take the values of Ra=10^3, 10^4 and 10^5, three dominant vertical circulations one of each on the left middle and right zones of the cavity almost completely swept. The shapes can be simulated for the three values quoted, a slight deformation is observed at the extremities of the vortices with the increase in the number of Rayleigh Ra=10^6.

Figures (4), (7) , (10) and (13), present the variation of the local Nusselt number compared to the cold wall of height and the bottom hot wall for different Rayleigh numbers, the variation is more seen for hot walls which explains the higher temperature effect.

**** Linear heating of the bottom wall with fins**

The contours of isotherms, current functions and iso-velocities are represented in figures (5), (8), (11) and (14) for Ra = 10^3-10^6 and Pr = 0.71 when the bottom wall is heated in a non-uniform linear manner, the non-uniform heating suppresses singularities at the edges of the bottom wall and presents regular temperature distribution throughout the cavity.

For Ra = 10^3 and Pr = 0.7 (Figure 5), the thermal boundary layer develops more than 70% of the cavity, which is lower compared to the case of uniform heating, it is observed in the around Ra =10^4 (Figure 8). It can be noted that the temperature at the bottom wall is not uniform and a temperature maximum occurs at the center. Therefore, higher rates of heat transfer occur at the center.

At Ra = 10^5(Figure 11), due to non-uniform bottom heating, the heating rate near the wall is generally lower, which induces less buoyancy resulting in a lower thermal gradient throughout the domain.

The uniformity of the temperature distribution and the temperature gradient are even less observed on the regime of the central part inside the upper half of the domain. The effect of lower buoyancy also leads to a large zone of temperature stratification at the vertical line of symmetry.

From $Ra = 10^6$ (Figure 14), the mechanism of convection becomes more pronounced and therefore the central vortex moves upwards. We also notice that the isotherms are horizontal and vertical inside the enclosure, the boundary layers become very thin, this can be attributed to a current inside the cavity which also causes a reduction in temperature gradients in the center of the high convection cavity.

The contours of the iso-velocity reveal several important characteristics, in the contours of the iso- velocity-*u*, for the values of $Ra=10^3$, 10^4 and 10^5, we notice four main horizontal vortices form above the fins, two other secondary ones form at the bottom of the cavity above the hot wall. For the value of $Ra=10^6$, two main vortices move away upwards towards the adiabatic wall while in the rest of the cavity several secondary vortices form around the fin.

For the contours of the iso-velocity-*v*, if we take the values of $Ra=10^3$, 10^4 and 10^5 three dominant vertical circulations one of each on the left middle and right zones of the cavity almost completely swept. The gaits can be simulated for the three values quoted, a slight deformation is observed at the extremities of the vortices with the increase in the number of Rayleigh $Ra=10^6$.

It should be noted that the presence of the fins has only slightly influenced the temperature, streamlines or iso-velocities, the change is only observed in the vicinity of the fins.

We present below the average Nusselt number variation for top and bottom walls, as function of Rayleigh number for different number of fins.

Figure 15 shows the evolution of the average Nusselt number with respect to the Rayleigh number for different numbers of fins with h/H = 0.20 and w/W = 0.05 on the hot and cold horizontal walls respectively.

As shown in the figure, the Nusselt number increases with increasing Rayleigh number for a number of fins ranging from 0 to 7 fins. The maximum values of the Nusselt number are reached for the case with three fins near the hot side of the cavity, on the other hand, the maximum values of the Nusselt number are reached for the case with seven fins near the cold side of the cavity.

Figure 16 illustrates the variation of the average Nusselt number function of the number of fins. Notice that the maximum value of the average Nusselt number is reached for the case with three fins near the hot side of the cavity at $Ra=10^6$, however it is reached at seven fins near the cold wall.

Figure 17 shows the evolution of the average Nusselt number in according with the height of the fin for different numbers of fins, as shown in the figure. Note that the average Nusselt number is reached for the case of two and three fins near the hot side of the cavity at h/H=3/5, contrary to the case of the cold wall, it is reached at two, tree and seven fins with h/H=3/5. The average Nusselt number variation for the top and bottom wall is presented below, as function of the number of fins for different Rayleigh numbers.

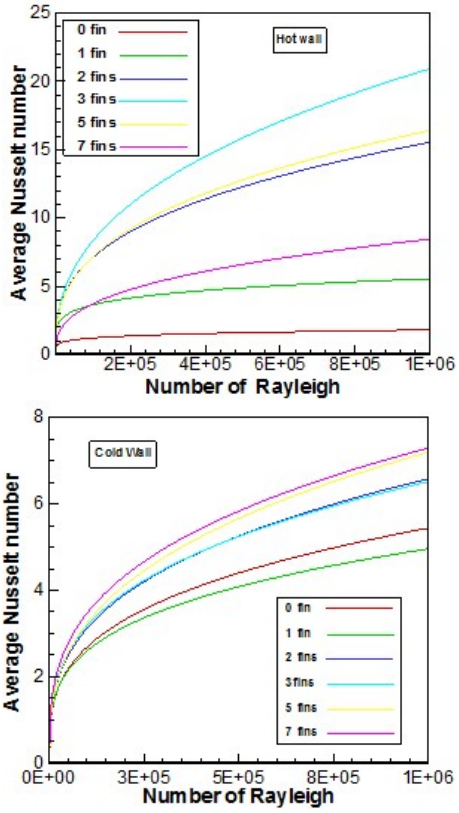

Fig. 15: Average Nusselt number according to Rayleigh number

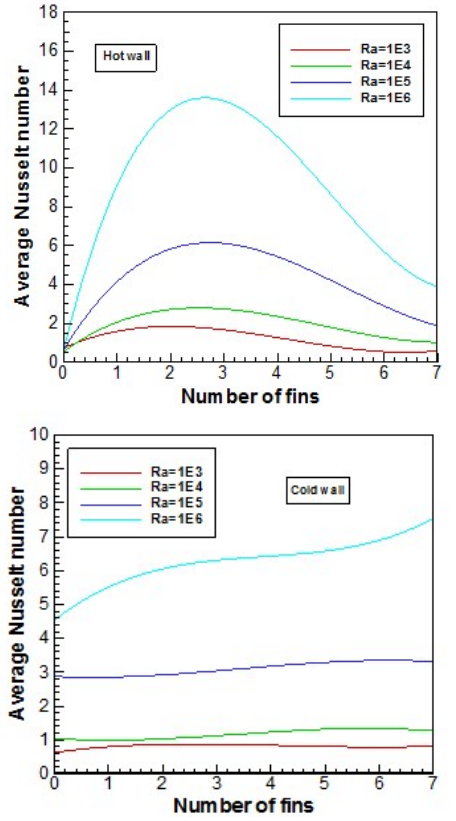

Fig.16: Average Nusselt number according to the number of fins

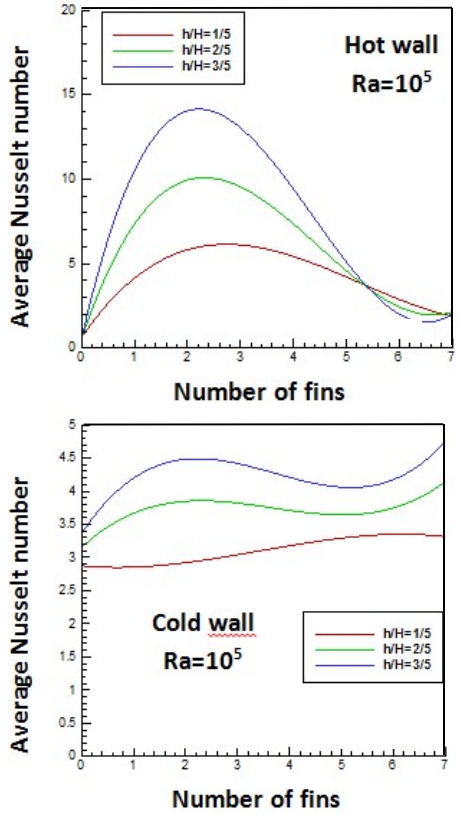

Fig. 17: Average Nusselt number at Ra=10^5 in according with the height of the fin

IX. Conclusion

A numerical study has been performed to investigate natural convection in a square cavity for laminar flow case. The cavity is made up of a finite number of fins on the bottom wall whose purpose is to improve the overall rate of heat transfer. The fins are heated using a non-uniform linear temperature profile; the vertical walls are adiabatic while the horizontal walls are subjected to cold temperatures at the top walls and hot and non-uniform temperatures at the bottom. The finite volume method is used for solving the governing equations. This method allows to obtain more realistic solutions in terms of isotherms, current functions as well as iso-velocities for a wide range of Rayleigh number and a Prandtl number fixed at 0.71.

The heat transfer rate is lower at the edges by the non-uniform heating, while it exhibits higher heat transfer rates at the center of the bottom wall. Boundary layer formation has been shown to occur, thermal boundary layer has been observed to grow about 60% for non-uniform heating. Non-uniform heating can be used in small regimes followed by uniform heating. This combination can be suitable to achieve improved heat transfer effects The results obtained are also very useful for a better understanding of heat transfer by natural convection which takes place in partitioned enclosures, and towards the best and cheapest way to achieve thermal performance of these heat transfer elements.

Finally, we would like to stress the idea that the modeling of a heat transfer or a fluid flow system must be guided by the objectives and the constraints of the system.

References

[1] Wu-Shung Fu and Wen-JiannShieh; "A penalty finite element method for natural convection heat transfer in a partially divided enclosure".Int. Comm. Heat Mass Transfer, Vol. 15, pp. 323-332, 1988

[2] Milos H. Novak and Edwin S. Nowak; "The CAV program for numerical evaluation of laminar natural convection heat transfer in vertical rectangular cavities".Computer Physics communications 78 (1993) 95-104 North-Holland.DOI: 10.1016/0010-4655(93)90145-3.

[3] Dagtekin and H.F. Oztop; "Natural Convection Heat Transfer By Heated Partitions WithinEnclosure".International Communication Heat Mass Transfer; Vol 28, No. 6, pp. 823-834. 2001. DOI: 10.1016/S0735-1933(01)00286-X.

[4] N. Yucel, A.H. Ozdem; " Natural convection in partially divided square enclosure", Heat and Mass Transfer 40 (2003) 167–175. DOI: 10.1007/s00231-002-0361-4.

[5] E. Bilgen; Natural convection in cavities with a thin fin on the hot wall.
International Journal of Heat and Mass Transfer 48 (2005) 3493–3505. DOI: 10.1016/j.ijheatmasstransfer.2005.03.016.

[6] Ahmed Al-Fahaid;"Numerical study of conjugate heat transfer in enclosures with fins attached to a vertical sidewall". Kuwait J. Sc. Eng. 33(2) pp 205-208, 2006.

[7] A. Ben-Nakhi; A. J. Chamkha; "Conjugate natural convection in a square enclosure with inclined thin fin of arbitrary length". International Journal of Thermal Sciences 46 (2007) 467–478. DOI: 10.1016/j.ijthermalsci.2006.07.008.

[8] A. Al Amiri; K. Khanafer; I. Pop; "Buoyancy-induced flow and heat transfer in a partially divided square enclosure".International Journal of Heat and Mass Transfer 52 (2009).3818–3828. DOI:10.1016/j.ijheatmasstransfer.2009.01.043.

[9] V.A.F. Costa ; "Natural convection in partially divided square enclosures: Effects of thermal boundary conditions and thermal conductivity of the partitions". International Journal of Heat and Mass Transfer, Volume 55, Issues 25–26, December 2012, Pages 7812-7822. DOI: 10.1016/j.ijheatmasstransfer.2012.08.004.

[10] FatihSelimefendigil, Hakan F. Öztop; "Fuzzy-based estimation of mixed convection heat transfer in a square cavity in the presence of an adiabatic inclined fin". International Communications in Heat and Mass Transfer 39 (2012) 1639–1646. DOI:10.1016/j.icheatmasstransfer.2012.10.006.

[11] ChahrazedBenseghir,SamirRahal; "Simulation of heat transfer in a square cavity with two fins attached to the hot wall". Energy Procedia 18,(2012), 1299 – 1306. DOI: 10.1016/j.egypro.2012.05.147.

[12] Semen G. Martyusheva , Mikhail A. Sheremeta; "Conjugate natural convection combined with surface thermalradiation in an air filled cavity with internal heat source". International Journal of Thermal Sciences 76, (2014), 51-67. DOI:10.1016/j.ijthermalsci.2013.08.012ISBN: 1290-0729

[13] M. Sathiyamoorthy ,TanmayBasak , S. Roy , I. Pop; "Steady natural convection flows in a square cavity with linearly heated side wall(s)". International Journal of Heat and Mass Transfer 50, (2007), 766–775.

[14] D. C. Wan, B. S. V. Patnaik, and G. W. Wei "A new Benchmark quality solutionfor the buoyancy-driven cavityby discrete singular convolution". Numerical Heat Transfer, Part B, 40: 199- 228, 2001. DOI :10.1080/104077901752379620.

[15] G. Barakos , E. Mitsoulis and D. Assimacopoulos; "Natural convection flow in a square cavityRevisited: laminar and turbulent models withWall functions". International Journal For Numerical Methods In Fluids, Vol. 18, 695-719 (1994). DOI:10.1002/FLD.1650180705

[16] D. de Vahl Davis, "Natural Convection of Air in a square Cavity : A Bench Mark Solution",Int., J., Numer. Meth. Fluids, Vol. 3, pp. 249-264, 1983. DOI:10.1002/fld.1650030305.

Mohamed Tarek ATTOUCHI graduated in mechanical engineering in 1995 and received the Magister degree in 2005 mechanical engineering from the Ecole Nationale Polytechnique, Algiers, Algeria. He is an Assistant Professor at Ecole Nationale Polytechnique since 1990.